Available online at www.sciencedirect.com
SCIENCE DIRECT®
Corrosion Science 46 (2004) 955–977
CORROSION SCIENCE
www.elsevier.com/locate/corsci

Galvanic corrosion of magnesium alloy AZ91D in contact with an aluminium alloy, steel and zinc

Guangling Song [a,*], Birgir Johannesson [b], Sarath Hapugoda [a], David StJohn [a]

[a] *CRC for Cast Metals Manufacturing (CAST), Department of Mining Minerals and Materials Engineering, Division of Materials Engineering, School of Engineering, The University of Queensland, St. Lucia, Brisbane, QLD 4072, Australia*
[b] *Materials and Environmental Department, Technological Institute of Iceland, Keldnaholt, 112 Reykjavik, Iceland*

Received 17 January 2003; accepted 2 July 2003

Abstract

An investigation was carried out into the galvanic corrosion of magnesium alloy AZ91D in contact with zinc, aluminium alloy A380 and 4150 steel. Specially designed test panels were used to measure galvanic currents under salt spray conditions. It was found that the distributions of the galvanic current densities on AZ91D and on the cathodes were different. An insulating spacer between the AZ91D anode and the cathodes could not eliminate galvanic corrosion. Steel was the worst cathode and aluminium the least aggressive to AZ91D. Corrosion products from the anode and cathodes appeared to be able to affect the galvanic corrosion process through an ''alkalisation'', ''passivation'', ''poisoning'' effect or ''shortcut'' effect.

Keywords: A. Magnesium

* Corresponding author. Tel.: +61-7-3365-4167; fax: +61-7-3365-3888.
E-mail address: g.song@minmet.uq.edu.au (G. Song).

0010-938X/$ - see front matter © 2003 Elsevier Ltd. All rights reserved.
doi:10.1016/S0010-938X(03)00190-2

1. Introduction

Magnesium alloys are being increasingly used in the automotive, aerospace and electronics industries. Considerable effort is being expended to further reduce fuel consumption and hence environmental pollution through replacing existing aluminium components with even lighter magnesium parts in automobile applications. An example of such effort was in the early 1980s when Volvo conducted a ''Light Component Project'', which resulted in a concept car [1,2].

Galvanic corrosion is one of the major obstacles to the use of magnesium parts in the automobile industry, and has been identified as a key issue if magnesium is used in exterior components in a vehicle [3]. This is because magnesium is the most active metal in the galvanic series [4], and a magnesium alloy component is always the active anode if it is in contact with other metals. Theoretically, galvanic corrosion can be eliminated by insulating or blocking the direct electrical contact between the magnesium alloys and other metals. Unfortunately, in practice direct contacts are required or unavoidable in the vehicle design because of mechanical and electrical demands.

In corrosion science and protection engineering, galvanic corrosion is an important topic. Numerous publications have laid a solid theoretical background in this area [5–8]. The galvanic corrosion rate is basically determined by:

$$i_g = (E_c - E_a)/(R_a + R_c + R_s + R_m) \tag{1}$$

where i_g is the galvanic current between the anode and the cathode, E_c and E_a are the open circuit potentials of the cathode and anode, R_c and R_a are the cathode resistance and anode resistance respectively, R_s is resistance of the solution between the anode and cathode, and R_m is the metal resistance from the anode surface to the cathode surface through a metallic path. Normally R_m is negligible if the two electrode metals are in a direct electrical contact. Any factor that can affect these parameters will influence the galvanic corrosion rate.

Eq. (1) is a theoretical or conceptual relationship. In practice, there are complicated interactions among these factors. For example, R_s depends on the geometric shape of the solution path between the anode and cathode. The distributions of current density and potential are always closely related to the geometric shape of the system. Therefore, the estimation of galvanic current or galvanic current density sometimes is very difficult for a practical system. Only for a galvanic corrosion specimen with a very geometry, can the analytical prediction of galvanic current density or distribution of galvanic current density be possible [7,9–16]. Usually, numerical techniques and computer modelling have to be used [17–28] for a complex geometric system and the numerical approach has become a trend in galvanic corrosion research recently.

Recent numerical and computer modelling techniques, which have been used for conventional metals, require polarisation curves as the boundary conditions in solving the governing equation. However, most magnesium alloys have a special electrochemical behaviour, the so-called ''negative difference effect'' [29,30]

and their polarisation behaviour is different from conventional metals in most environments. The special polarisation behaviour of magnesium alloys can lead to special boundary conditions. Therefore, whether those models developed for the conventional metals are applicable to magnesium alloys needs to be validated.

Limited publications on the galvanic corrosion of magnesium alloys [3,31–37] have indicated that current research interest is mainly focussed on the compatibility of the materials (including fasteners) with magnesium components. In those studies, only the overall galvanic corrosion performance of the magnesium alloy was evaluated based on the measured weight loss, the penetration depth, the total galvanic current or even the visual observation of the corrosion damage on the whole magnesium component. No detailed measurements of the distribution of galvanic current density have been made. However, the distribution of galvanic current density is essential information from the design point of view. The design of a reasonable prevention measure or the geometric shape of a component requires information on the width of the galvanically affected zone, the effectiveness of a coating in depressing the galvanic current, and how the distribution of galvanic current density is altered by inserting an insulating washer, etc. Moreover, in future the experimentally measured distribution of galvanic current density is essential information for validation of the galvanic corrosion models particularly developed for magnesium alloys. Therefore, measuring and understanding the reasons for the distribution of the galvanic current density on magnesium alloys coupled with other metals is of significance.

Accurate measurement of galvanic corrosion is difficult under a thin aqueous film. Automotive components are mainly exposed to various atmospheric conditions, including high humidity rain, snow and salt water. Galvanic corrosion occurs in these cases under a very thin aqueous electrolyte. Conventional electrochemical techniques employing a large amount of electrolyte will introduce significant errors under the think electrolyte film condition [8]. Recently, a Kelvin probe technique has been used to measure the surface potential distribution [8,38,39]. However, this technique requires sophisticated equipment, and the measured results are the surface potentials, not the galvanic current densities. Some theoretical errors could be introduced in the conversion of the potentials into galvanic current densities or galvanic corrosion rates.

In this paper, the distributions of galvanic current densities are measured with specially designed test panels, and several issues are addressed based on the measurements, such as the development of galvanic corrosion with time, the distribution of galvanic current density, the extent of the galvanically affected zone, the influence of the ratio of anode area to cathode area, the compatibility between cathode and anode materials and the effects of corrosion products from anode and cathode. It is hoped that the study will lead to an improved understanding of the galvanic corrosion of magnesium and its alloys and the results will assist in the understanding of the general corrosion performance of magnesium alloys, which is closely related to the microgalvanic effect caused by the different phases and impurities in the alloys.

2. Experimental

2.1. Materials

Four types of materials were used in these experiments: AZ91D magnesium ingot, 380 aluminium alloy, 4150 high strength steel and pure zinc of 99.95% purity. AZ91D was chosen because it is the most widely used magnesium alloy. Al380 has a composition and microstructure typical of aluminium alloys used in car engine blocks. Steel 4150 is a bolt and washer material, and zinc is often present on the surface of galvanised steels. All these non-magnesium based materials are commonly used and in practice magnesium alloys will unavoidably be in contact with them in practice.

2.2. Test panels

Specially designed test panels were used to measure the distribution of galvanic corrosion current density under the standard salt spraying condition. The configuration of the test panels is shown in Fig. 1. Each test panel consists of 10 or 20 metal plates. The plates were AZ91D, aluminium alloy, zinc and steel. Each plate had a cross-section of 3 mm × 15 mm. An interval of 2 mm between the plates was carefully maintained to avoid direct electrical contact between the plates. All the plates were moulded in epoxy with wire connections submerged in the epoxy resin. The cross-sections of the plates were exposed for salt spray testing.

In this paper, "Mg" is AZ91D, "Al" refers to Al380 alloy, "steel" stands for steel 4150 and "Zn" means pure zinc. The number in front of "Mg", "steel", "Al" or

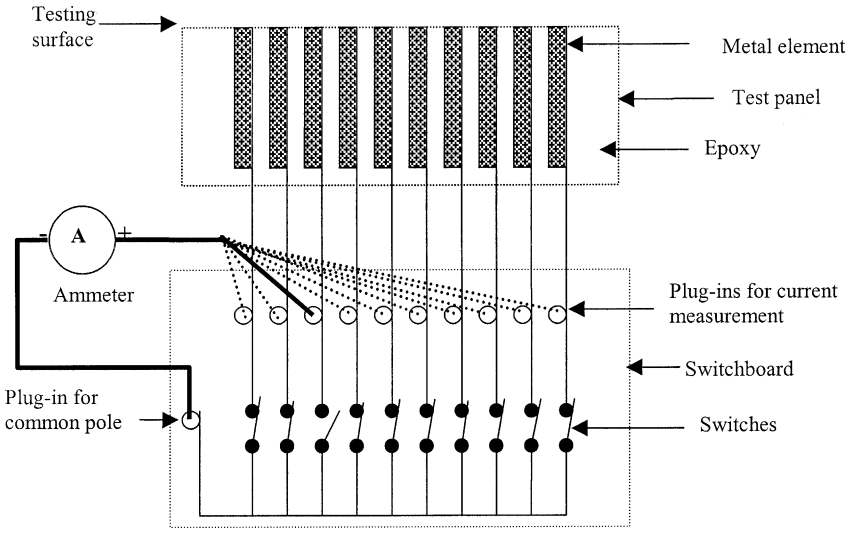

Fig. 1. Configuration of the test panel and switchboard for the measurement of galvanic current.

''Zn'' denotes the number of metal plates used in constructing the test panels. For example, test panel ''5Mc–5Mg'' means that this test panel consists of 5 plates of ''Mc'' and 5 plates of ''Mg''. ''Mc'' represents a coupling cathode which can be zinc, steel 4150 or Al380. Test panels with different numbers of plates of ''Mc'' and ''Mg'' were used to represent galvanic couples with different ratios of cathode area to anode area.

A test panel with 10 plates of AZ91D (no other metal plates) was used to identify the background current. The current fluctuated across this test panel in the salt spraying chamber randomly within the range of 0 to ± 22 $\mu A/cm^2$. Therefore, only currents with absolute values greater than 22 $\mu A/cm^2$ were taken as galvanic currents.

Some electrodes were also made from the above materials AZ91D, steel 4150, Al380 and zinc for measurements of their polarisation behaviour. The metals were machined into 1 cm^3 cubic coupons. After connection of electrical lead wires to the coupons, they were embedded in epoxy resin. One unsealed surface was used as the testing surface in the electrochemical measurements.

2.3. Testing solutions

5% NaCl solution was used for the galvanic corrosion testing in a salt spray chamber. In addition, some other chemicals ($Mg(OH)_2$, ZnO, $Al(OH)_3$, and $FeCl_3$) were sometimes added to the salt solution when measuring polarisation curves. All the solutions were prepared with demineralised water and AR grade chemicals.

2.4. Measurement of galvanic currents

To measure the galvanic current of each plate without electrically disconnecting the plate from the circuit, a ''switchboard'' was made (see Fig. 1). During the measurements, all the switches were ''on'', so all the plates were electrically connected. Before the measurement of the current from a plate started, an ammeter was connected to the switchboard between the ''plug-in for common pole'' and the ''plug-in for current measurement'' and then the corresponding switch was set to ''off''. This allowed the current from the plate to pass through the ammeter. After the current from that plate was measured, the switch was set to ''on''. The ammeter was then disconnected from that ''plug-in'' and connected to the next ''plug-in'' for the next plate. In this way, no plate was disconnected from the circuit during the measurement, i.e., all the plates in a test panel during galvanic current measurements were kept electrically connected.

2.5. Salt spraying

Salt spray testing was conducted according to the standard ASTM B117. The exposed surface of each test panel was tilted 15° to the vertical in the chamber. During the test the galvanic current was measured on the switchboard outside the chamber.

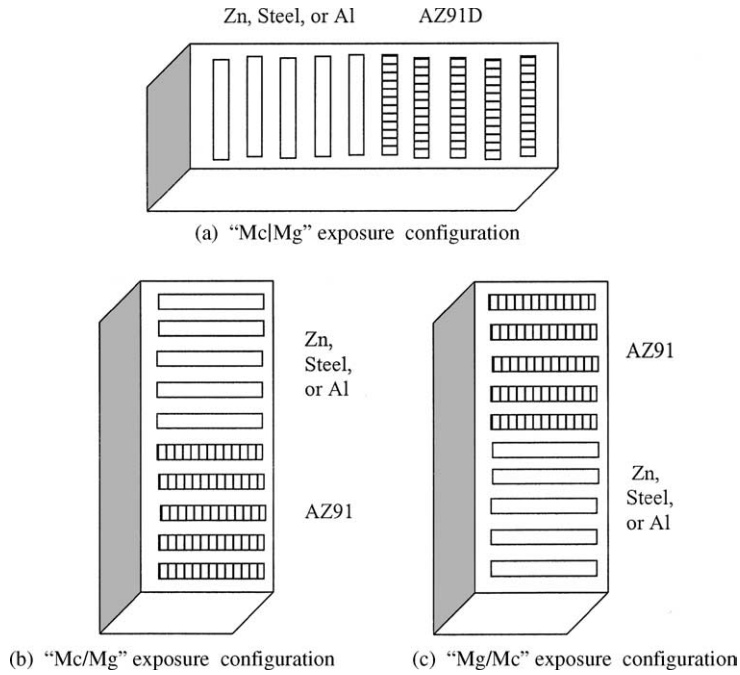

Fig. 2. The exposure configurations of test panels used in the salt spraying chamber, "Mc" stands for steel 4150, Al380 or zinc.

To investigate the influence of the relative positions of anode and cathode, some test panels were mounted in three different configurations, "Mc|Mg", "Mc/Mg" and "Mg/Mc" (Fig. 2). The normal placement of a test panel in the chamber for most tests was the "Mc|Mg" exposure configuration (Fig. 2(a)). In this case, AZ91D and its coupling cathode were placed side by side at the same horizontal level. The corrosion products of AZ91D and its coupling cathode was flushed down to the bottom of the test panel by the sprayed salt solution, ensuring that corrosion products from either anode or cathode would not contaminate each other. In the "Mc/Mg" (Fig. 2(b)) exposure configuration, the cathode plates were below AZ91D, while in the "Mg/Mc" (Fig. 2(c)) exposure configuration the cathode plates were on the top of AZ91D. In these exposure configurations ("Mg/Mc" and "Mc/Mg"), the corrosion products of the electrode on the top could flow down to the surface of the bottom electrode.

2.6. Polarisation curve

The polarisation curves of the couples were measured in an electrolytic cell containing about 500 mL solution using a Solatron 1287 + 1255B electrochemical measurement system. The polarisation of AZ91D started from a cathodic potential, about −300 mV relative to its corrosion potential, and stopped at an anodic current

density of about 1 mA/cm^2. For steel 4150, aluminium 380 and zinc, the initial polarisation potentials were +300 mV relative to their corrosion potentials and the polarisation stopped at a cathodic current density of about −1 mA/cm^2. In all polarisation measurements the potential scanning rate was 10 mV/min and all the potentials were relative to a silver/silver chloride reference electrode.

All the above mentioned measurements were performed at 25 ± 1 °C.

3. Results and discussion

3.1. Development of galvanic corrosion

The development of galvanic corrosion can be shown by the change in average galvanic current or current density over the whole AZ91D anode surface with time. A typical result is presented in Fig. 3. The most important feature shown by Fig. 3 is that the galvanic current increases steadily with time in the first few hours. After that, the current fluctuates around a value within a certain range. Changing the cathode metal or ratio of cathode area to anode area did not change this feature. These changes only led to different absolute values of the galvanic currents.

The initial increase in galvanic current could be related to the roughening (increase in area) of test panel surface caused by corrosion. The fluctuation of the galvanic currents can be interpreted as competition between the initiation and ceasing of corrosion in various areas. It is possible that corrosion stopped in a corroded area, but was initiated in a new area.

The fluctuations and incubations involved in the galvanic corrosion of AZ91D suggest that prediction of long-term galvanic corrosion behaviour will be difficult, if the prediction is based only on short-term tests. In real service environments, due to the complicated changes in factors such as temperature, humidity and the

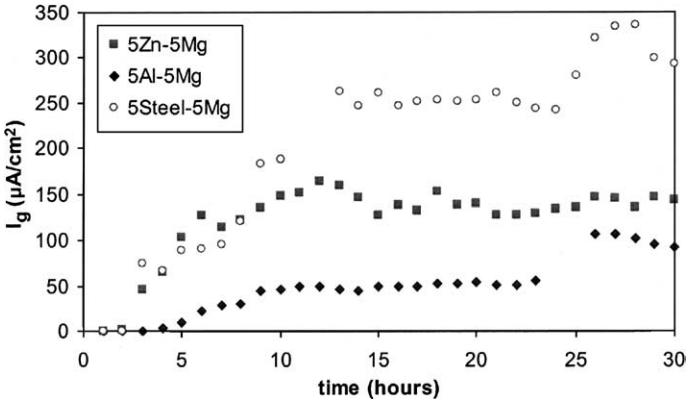

Fig. 3. Typical change in average galvanic current density with time for "5Mc–5Mg" test panels in the "Mc|Mg" exposure configuration.

constituents of the exposing media, precise prediction of galvanic corrosion rates is even more difficult and may be in effect impossible.

3.2. Distribution of galvanic current density

Due to the increasing solution resistance between these two coupled materials [40], the galvanic current density should be much higher in the area adjacent to the coupling metal than in an area farther away. Fig. 4 shows typical distributions of the galvanic current density on the test panels ''5Al–5Mg'', ''5Zn–5Mg'' and ''5steel–5Mg''. The galvanic current densities on both the magnesium side and the coupling cathode metal side decrease with increasing distance from the ''anode|cathode'' junction. This indicates that galvanic corrosion was more severe on magnesium in the area adjacent to the cathode, while the cathode metal was better protected from corrosion attack in the area adjacent to the anode.

The decrease of the galvanic current density with increasing distance (x) from the ''anode|cathode'' junction is non-linear (Fig. 4). It seems to be an exponential function of the distance x. An exponential distribution of galvanic current density (I_g) with distance x has been reported [8] for a ''Fe–Zn'' couple under a thin aqueous film:

$$I_g = I_0 \exp(-x/L) \tag{2}$$

where

$$L = (R_p/\rho_s)^{1/2} \tag{3}$$

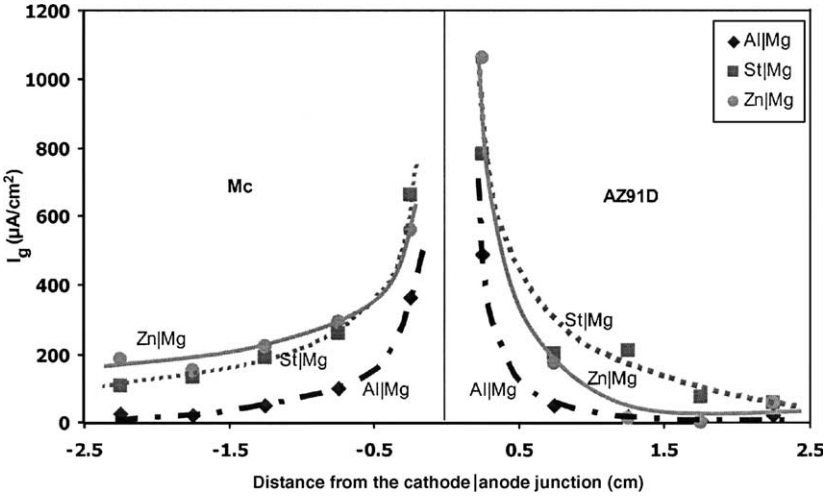

Fig. 4. The distribution of galvanic current densities on the ''5Mc–5Mg'' test panels in the ''Mc|Mg'' exposure configuration after 2 h and 40 min of salt spray testing.

$$I_0 = V_0/(R_p\rho_s)^{1/2} \tag{4}$$

V_0 is the potential at the junction point, $E_a < V_0 < E_c$. R_p is the polarisation resistance per unit length of the anode or cathode, and ρ_s is the solution resistance per unit length or resistivity of the aqueous thin film on the test panel surface. L can be regarded as a measure of the effective distance that significant galvanic current can occur on the test panel surface. A higher R_p or a lower ρ_s would lead to a smaller L, and thus a wider distribution of galvanic current. A narrow distribution of galvanic current means a small R_p or a low conductivity of the solution. All these are consistent with what the Wagner parameter [41–43] signifies. According to Eq. (2), $\mathrm{Ln}(I_g)$ should be linearly dependent on x:

$$\mathrm{Ln}(I_g) = \mathrm{Ln}(I_0) - x/L \tag{5}$$

A higher slope is equivalent to a narrower galvanic current distribution.

To examine the exponential distribution, Fig. 4 is replotted to show the dependence of $\mathrm{Ln}(I_g)$ on x, and the results are presented in Fig. 5. The current densities data can approximately be correlated with straight lines.

Fig. 5 thus indicates that the galvanic current densities approximately follow the exponential distributions. It should be borne in mind that the theoretical exponential equation (Eq. (2)) was deduced based on the transmission line model under the half indefinite condition with an assumption that polarisation resistance R_p is a constant that is independent of the distance, current density or potential. In fact, this assumption is not reasonable, because polarisation resistance strongly depends on polarisation current density or potential and thus distance x. Therefore, the deduced

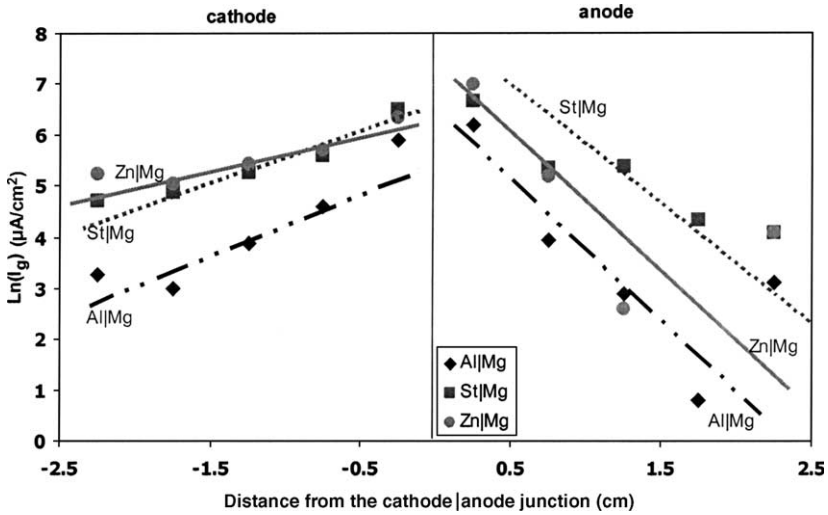

Fig. 5. The dependence of $\mathrm{Ln}(I_g)$ on the distance from "anode|cathode" junction, calculated from Fig. 4.

theoretical distribution of the galvanic current density over the test panel surface may not be accurate.

Another feature of Fig. 4 is that the galvanic current density decreases more dramatically with distance (x) from the junction on the ''Mg'' side than on the ''Mc'' side. In other words, AZ91D has a narrower distribution of higher galvanic current density than its coupling cathode. Such differences are reflected in Fig. 5, where the straight lines on the ''Mg'' side are all correspondingly steeper than those on the ''Mc'' side.

The different distributions of galvanic current densities on the cathode and anode can be attributed to the different polarisation behaviours of the anode and the cathode. The polarisation curves of AZ91D, steel 4150, Al380 and zinc in 5% NaCl are shown in Fig. 6. The anodic polarisation curve of AZ91D is almost a vertical straight line, which means that R_p of AZ91D is very small. The cathodic polarisation curves for steel, Al, and Zn are relatively complicated. The limiting diffusion current due to oxygen diffusion is apparent close to the corrosion potentials of the cathodes. Hydrogen evolution is responsible for the increase in current as the polarisation potential becomes more negative. Zn, Al and Fe have different hydrogen overvoltages. So significant increases of the cathodic currents start from different potentials for these metals. Most importantly, all the cathodic polarisation curves of the cathodes are overall much flatter than the anodic polarisation curve of AZ91D. In other words, the average cathodic polarisation resistances of these cathodes are much higher than the anodic polarisation resistance of AZ91D. Since the solution resistivity is almost the same in the tests, according to Eq. (3), the slopes of the straight lines on the ''Mc'' side should be smaller than that on the ''Mg'' side in Fig. 5. This explains the differences in the distributions of the anodic and cathodic current densities (Fig. 4).

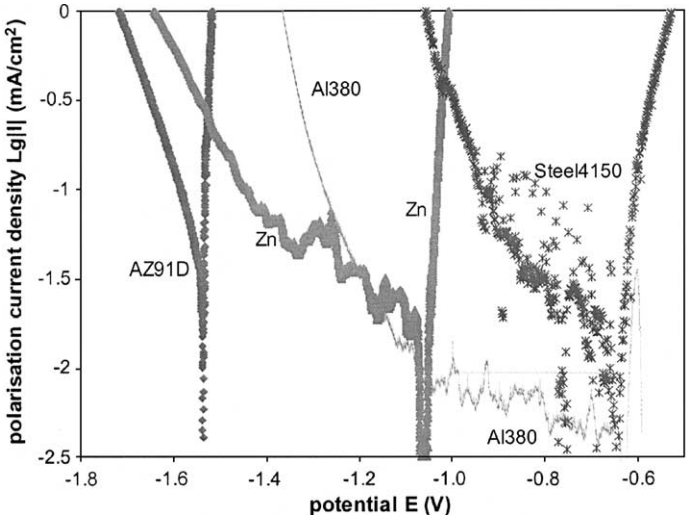

Fig. 6. Polarisation curves of AZ91D, Al380, steel 4150, and zinc in 5% NaCl.

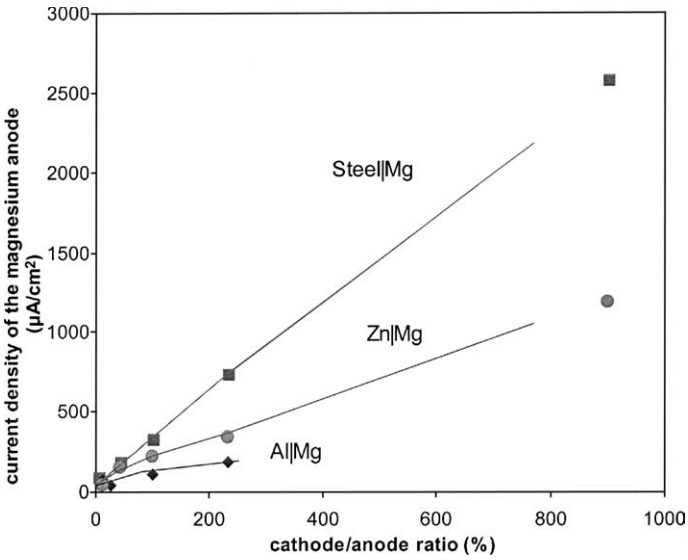

Fig. 7. Dependence of galvanic current on the cathode/anode ratio. The galvanic currents were obtained from test panels in the "Mc|Mg" exposure configuration after 2 days of salt spray testing.

3.3. Influence of coupling cathode metal

The dependence of the galvanic current density I_{ga} of the AZ91D anode on the ratio (r) of cathode area to anode area is shown in Fig. 7. Very clearly I_{ga} increases as r increases. The increase is most significant when AZ91D is in contact with steel, but it is not very remarkable for an Al|Mg couple.

The experimental results indicate that the worst combination for a galvanic couple is to have a high area ratio of steel to AZ91D. The area ratio, however, appears to affect the galvanic corrosion insignificantly when AZ91D is in contact with aluminium. These behaviours are consistent with the earlier experimental results (Figs. 3 and 4) in this study and the claimed comparability of Al, Zn and steel washers or fasteners with magnesium alloys in other publications [33,35,37]. For example, Starostin et al. [31] measured the galvanic corrosion currents and rates of AZ91 and AM50 coupled with cast iron, mild steel, Al6061, Zn, etc. in a 0.1% NaCl solution. The ratio of cathode area to anode area for the specimens in his study was 0.5. They found that at such a ratio steel was the worst coupling metal and Al and Zn coupling led to much lower galvanic corrosion rates. The results shown in Fig. 7 suggests that in a considerably wide range of the ratio of cathode area to anode area, steel is always the worst coupling cathode whilst aluminium the most mild in terms of their galvanic effect on magnesium anode.

The effects of coupling cathode metals on galvanic corrosion can be explained by referring to Eq. (1) and to the polarisation behaviours of AZ91D, A380, steel 4150 and zinc (Fig. 6). A larger difference between E_c and E_a, and a smaller R_c or R_a or R_s

can lead to a higher galvanic current. In this study, E_a, R_a and R_s did not change when AZ91D was coupled with different cathodes. This means that the different galvanic currents and the distributions of current densities were caused by different values of E_c and R_c in this case.

The galvanic current density of "steel|Mg" being higher than those of "Zn|Mg" and "Al|Mg" can be understood by comparing the polarisation curves of the cathode metals (Fig. 6). The cathodic polarisation current densities of steel 4150 are much larger than those of the other two cathodes Al380 and Zn, i.e., steel 4150 has a lower R_c. Meanwhile, the corrosion potential (E_c) of steel 4150 is more positive than those for Al380 and Zn. Therefore, according to Eq. (1), a lower I_g will result when AZ91 is in contact with steel 4150 than when in contact with Al380 or Zn.

It should be noted that even though the cathodic polarisation current densities of Al380 are lager than those of Zn (Fig. 6) when the polarisation potential is more negative than −1.2 V, Zn does have a slightly larger cathodic current than Al380 at less negative potentials. Therefore, if the solution resistance between anode and cathode is large enough, an "Al–Mg" couple could have a smaller galvanic current density than a "Zn–Mg" couple. Under the salt spraying condition, due to the small thickness of the liquid film on the test panel surface, solution resistance cannot be too small. So, it is quite possible that AZ91D in contact with Zn has a relatively larger galvanic corrosion rate than in contact with Al380.

3.4. Thickness of the insulating spacer between the anode and cathode

The effect of thickness (X) of the insulating spacer between AZ91D and the cathode metal on galvanic corrosion is shown in Fig. 8. The galvanic current decreases with the increase in the thickness of the insulating spacer. The decrease is more rapid over a smaller distance (around 1 cm) and then the decrease becomes slower as the thickness increases. Fig. 8 also shows that the measured currents are

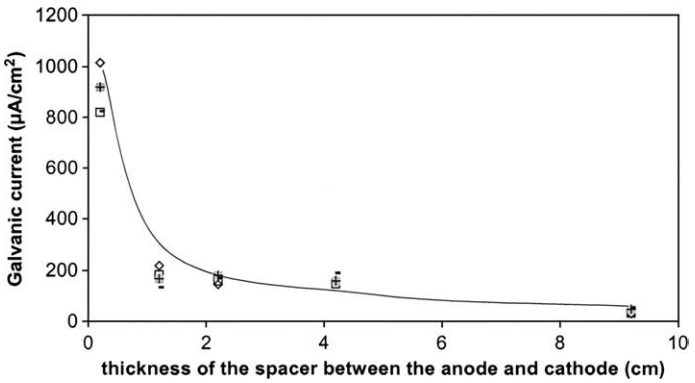

Fig. 8. Effect of thickness of the insulating spacer between the anode and cathode on the galvanic current. The galvanic currents were obtained from "1steel (N) 1Mg" test panels in "Mc|Mg" exposure configuration after 2 days of salt spray testing.

still higher than 22 μA/cm^2 with a thickness of the insulating spacer up to 9 cm, which means that galvanic corrosion can still occur under the salt spraying condition even though the thickness of the insulating spacer between AZ91D and steel is as wide as 9 cm.

It is noticed that the dependence of the galvanic current density on the thickness of the insulating spacer is non-linear. This is different from Hawke's results [33] that the galvanic corrosion indicated by the weight loss of diecast AZ91D plate was almost linearly dependent on the insulating spacer thickness, and based on the linear dependence, the galvanic corrosion could be eliminated if the spacer was thicker than 4.8 mm.

A simplified schematic diagram (Fig. 9) is drawn to elucidate the dependence of the galvanic current density on the thickness of the insulating spacer between the anode and cathode. In Fig. 9(A), E_a—A and E_c—C are typical anodic and cathodic polarisation curves of anode and cathode respectively. The difference in potential between the cathode and anode is presented as a curve B–E in Fig. 9(C). The potential drop across the solution between the anode and cathode is determined by the

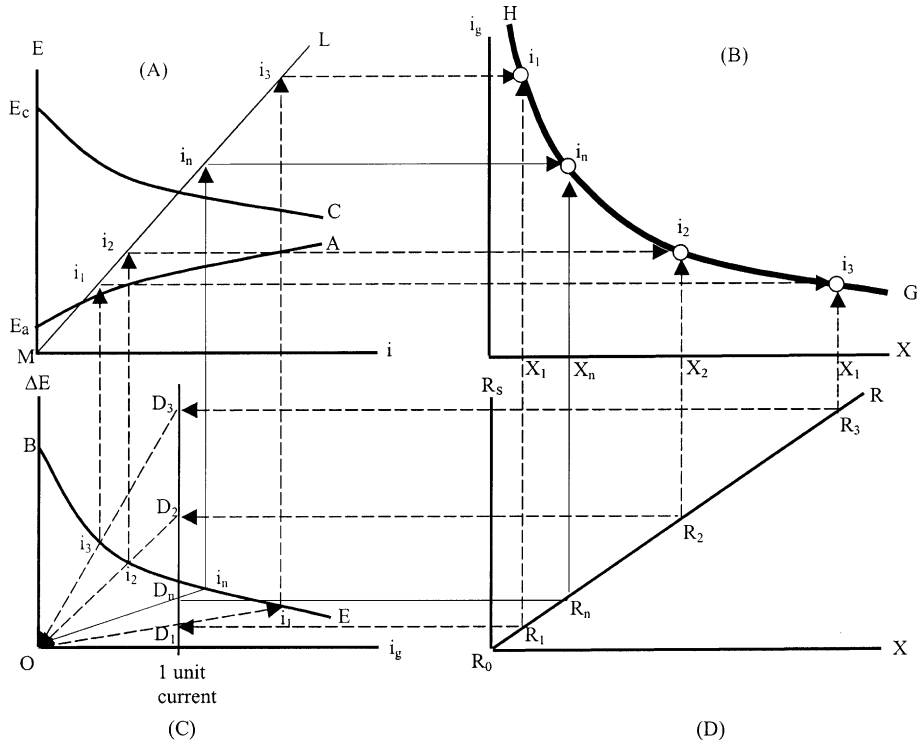

Fig. 9. Schematic diagram for the influence (X) of the spacer on the galvanic current (i_g). (A) Anodic and cathodic polarisation curves of the coupling anode and cathode, (B) dependence of galvanic current on thickness of the spacer, (C) the influence of galvanic current on the potential difference between the cathode and anode and the potential drop across the solution between the anode and cathode, (D) the relationship between solution resistance and the thickness of the spacer.

geometry of the solution. In this study, a uniform solution film was assumed to form on the surface of the test under the salt spraying condition. So the solution resistance should be a linear function of the thickness of the insulating spacer between the anode and cathode, which is plotted as a straight line R_0—R in Fig. 9(D). For a selected thickness X_n, the corresponding R_s is R_n. When a unit current passes through R_n, the potential drop across R_n will be D_n (Fig. 9(C)). The straight line O–D_n represents the dependence of the potential drop (D_n) across R_n on the galvanic current. The slope of O–D_n is R_n. Since the potential drop across the solution between anode and cathode is always equal to the potential difference between the cathode and anode, the interception point i_n between curve B–E and line O–D_n signifies the galvanic current when the thickness of the insulating spacer is X_n. The schematic relationship between galvanic current i_n and X_n can be obtained by transferring i_n and X_n from Fig. 9(C) and (D) into Fig. 9(B). The slope of line M–L in Fig. 9(A) is 1. The role of this line is to transfer the readings from the horizontal axis in Fig. 9(C) to the vertical axis of Fig. 9(B) whose horizontal axis is the thickness of the insulating spacer. Following these procedures, a thickness of the insulating spacer dependent galvanic current curve H–G can be plotted in Fig. 9(B). i_1, i_2 and i_3 on H–G are some example points.

From Fig. 9, it can been seen that curve G–H is eventually determined by E_c—C, E_a—A and R_0—R. Only if the second order differentials of the cathode and anode polarisation curves E_c—C and E_a—A are always equal at any current or potential, then G–H can be a straight line. In practice, this is almost impossible, as the anodic and cathodic reactions follow different mechanisms. Experimental polarisation curves (Fig. 6) have shown that the anodic current of the AZ91D anode increases more dramatically as potential becomes more positive than the cathodic currents of the coupling cathodes as potential becomes more positive. Based on these kinds of curves, galvanic current should decrease quickly with the thickness of the insulating spacer when the spacer is small, and the rate of decrease becomes slow as the thickness of the insulating spacer increases. The dependence of galvanic current on the thickness of the insulating spacer should be non-linear as shown in Fig. 8. The linear result in Hawke's work [33] could result from relatively low accuracy of their measurements. The galvanic corrosion rates in Hawke's work [33] were obtained through weight loss measurements, which could be influenced by general corrosion and could not be a sensitive method compared with the direct measurement of galvanic current as done here.

According to Fig. 9, G–H will not approach zero before X becomes infinite. This suggests that insertion of an insulating spacer may reduce galvanic corrosion significantly, but cannot eliminate it, because the insertion of an insulating spacer only increases the resistance of the aqueous film on the surface of the test panel, which retards the galvanic current. It does not block the electrical path in the solution.

3.5. Effect of galvanic corrosion products

In galvanic corrosion, several corrosion products will be generated which could in turn influence the galvanic corrosion process. One of the most obvious corrosion

products is Mg^{2+} ion dissolved from the anode. The corrosion of magnesium alloys will lead to an increase in pH value of the solution, the ''alkalisation effect''. Because of the alkalisation of the solution on the corroding magnesium surface (pH $\sim$ 11), it is even suspected that the adsorption of atmospheric CO_2 may occur during magnesium corrosion in the atmosphere [44,45]. The dissolution of magnesium leads to a reaction between Mg^{2+} and water (hydrolysis) and produces hydrogen from the magnesium surface and $Mg(OH)_2$ in the solution. The evolution of hydrogen leads to an increasing pH value of the solution before saturation with $Mg(OH)_2$ is reached. As the solubility of $Mg(OH)_2$ is very small, about 9 mg/L [46], the thin aqueous film on a corroding magnesium surface under atmospheric or salt spraying conditions can easily become saturated with $Mg(OH)_2$ by the rapid dissolution of magnesium.

The alkalised solution on the magnesium surface could influence the electrochemical behaviour of cathodes and hence galvanic corrosion. Figs. 10–12 show the distributions of the galvanic current densities of the ''5Mc–5Mg'' test panel in the ''Mc|Mg'', ''Mc/Mg'' and ''Mg/Mc'' exposure configurations (''Mc|Mg'', ''Mc/Mg'' and ''Mg/Mc'' are different exposure configurations, see Fig. 2). The galvanic current densities of the test panels in the ''Mg/Mc'' exposure configuration are all significantly lower than in the ''Mc|Mg'' exposure configuration, particularly in the regions adjacent to the ''anode|cathode'' junction.

The differences in corrosion caused by the different exposure configurations can be ascribed to the fact that the alkalised solution from the AZ91D anode surface can easily flow down to the cathode surfaces in the ''Mg/Mc'' exposure configuration, which could not happen in the ''Mc|Mg'' exposure configuration. Therefore, the smaller galvanic current densities of the test panels in the ''Mg/Mc'' exposure configuration can be attributed to the alkalisation of the solution on the cathode surfaces caused by the corrosion products coming from the anode surface.

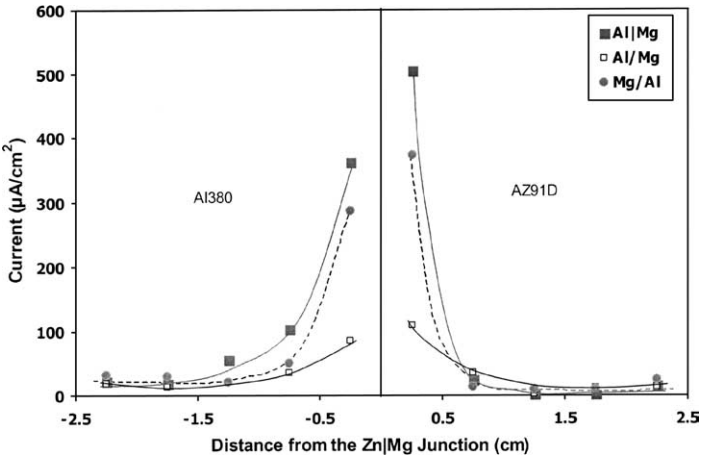

Fig. 10. The distribution of galvanic current densities on the ''5Al–5Mg'' test panel in the ''Mc|Mg'', ''Mc/Mg'' and ''Mg/Mc'' exposure configurations after exposure to salt spraying for 2 h.

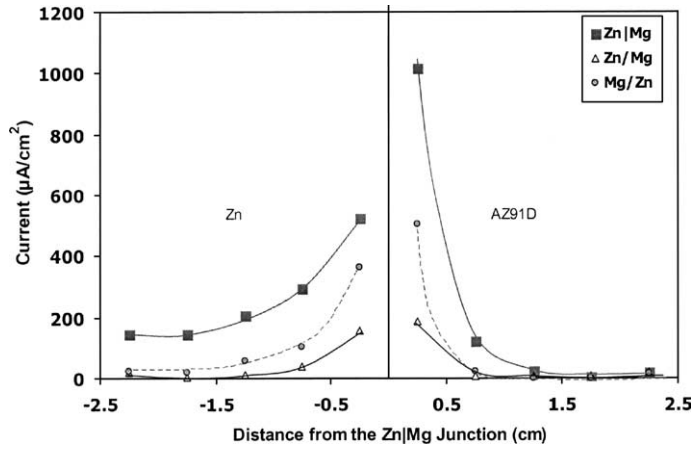

Fig. 11. The distributions of galvanic current densities on the "5Zn–5Mg" test panel in the "Mc|Mg", "Mc/Mg" and "Mg/Mc" exposure configurations after exposure to salt spraying for 2 h.

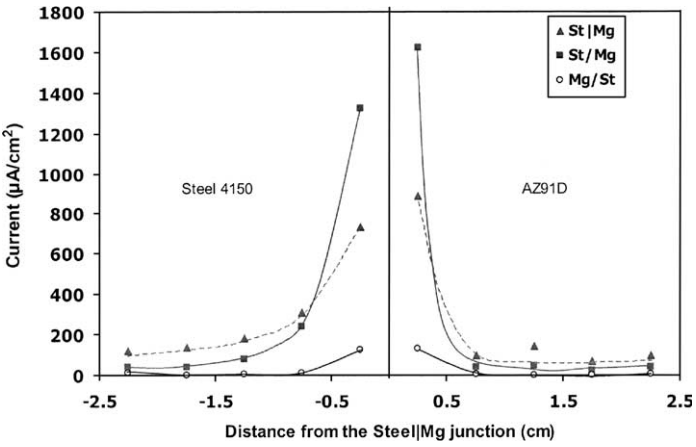

Fig. 12. The distributions of galvanic current densities on the "5steel–5Mg" test panel in the "Mc|Mg", "Mc/Mg" and "Mg/Mc" exposure configurations after exposure to salt spraying for 2 h.

To confirm whether the change in galvanic corrosion is caused by alkalisation of the solution, the polarisation curves of the cathodes (Fig. 13) were measured in $Mg(OH)_2$ saturated 5% NaCl. A normal 5% NaCl solution has a pH value around 7, while the $Mg(OH)_2$ saturated one was measured to be $pH = 10.8$. From Fig. 13, it can be seen that except for Zn, the decrease in cathodic currents of both Al380 and steel 4150 is significant by saturating NaCl with $Mg(OH)_2$. This means that the corrosion product $Mg(OH)_2$ can increase the cathodic polarisation resistance of these cathodes. Hence, if the cathode surfaces are alkalised by the AZ91D corrosion

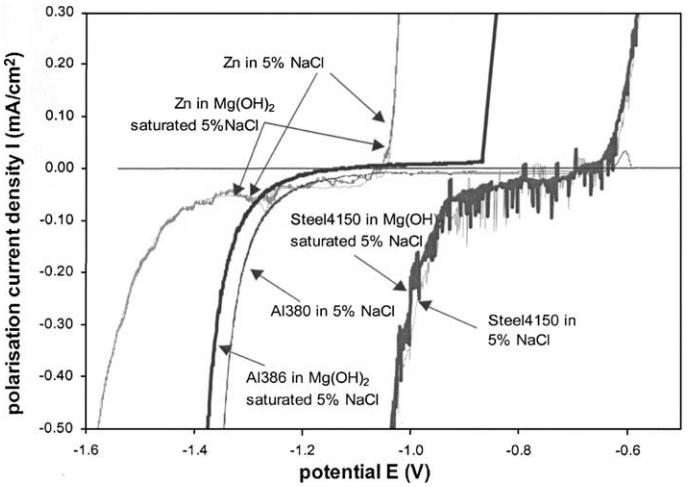

Fig. 13. Polarisation curves of Al380, steel 4150, and zinc in 5% NaCl and $Mg(OH)_2$ saturated 5% NaCl.

product, galvanic corrosion could becomes slightly less severe. This explains the differences in the galvanic current densities of the test panels between the ''Mc|Mg'' and ''Mg/Mc'' exposure configurations (Figs. 10–12). It is unclear why the decrease in the polarisation current density of Zn by $Mg(OH)_2$ is insignificant.

Figs. 10–12 also show another interesting phenomenon. Galvanic currents of the test panels in the ''Mc/Mg'' exposure configuration are evidentially different from those in the ''Mc|Mg'' exposure configuration. In the ''Mc/Mg'' exposure configuration galvanic corrosion became milder for ''5Al–5Mg'' and ''5Zn–5Mg'' test panels, but more severe for the ''5steel–5Mg'' panel. The reason for the difference could be that different corrosion products from the cathodes were flushed down to the anode surface, which affected the electrochemical behaviour of the anode, hence altering the galvanic corrosion performance of the test panels.

To illustrate the effect of corrosion products from the cathodes on the galvanic corrosion behaviour, several salt solutions, including 5% NaCl saturated with ZnO, 5% NaCl saturated with $Al(OH)_3$ and 5% NaCl + 0.1% $FeCl_3$, were used to simulate the solutions on corroding Zn, Al380 and steel 4150. The simulated solutions could be different from the real solutions in terms of their concentrations, but the main compositions should be the same. The electrochemical results of the AZ91D anode in these simulated solutions should be representative and be able to indicate the influence of the cathode products on electrochemical behaviour of the anode.

Fig. 14 displays the polarisation curves of AZ91D in these solutions. The changes in the polarisation curves by additions of ZnO, $Al(OH)_3$ and $FeCl_3$ are evident. The presence of ZnO or $Al(OH)_3$ in the salt solution results in a lower anodic polarisation curve. This implies that the galvanic current from AZ91D becomes smaller if the salt solution on the AZ91D surface is contaminated by ZnO or $Al(OH)_3$, consistent with the results shown in Figs. 10 and 11.

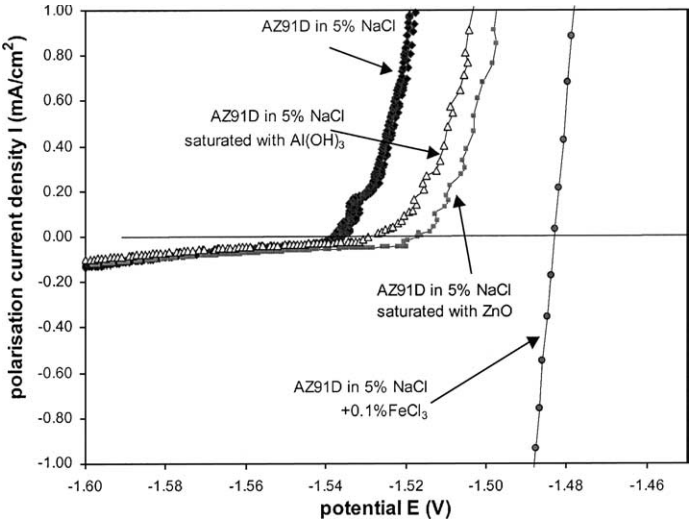

Fig. 14. Polarisation curves of AZ91D in 5% NaCl solutions saturated with $Al(OH)_3$ and ZnO, and in 5% NaCl solution + 0.1% FeCl.

The mechanism of the decrease in the galvanic current for "5Zn–5Mg" or "5Al–5Mg" in the "Mc/Mg" exposure configuration compared with that in the "Mc|Mg" exposure configuration is postulated as follows. Even though the galvanic effect offers some degree of cathodic protection for aluminium and zinc cathodes, the dissolution of these metals in the salt solution is still unavoidable, particularly in the region far away from the "anode|cathode" junction. This has been experimentally verified by the white corrosion products seen on most of the cathode plate surfaces after salt spraying. The dissolved Zn^{2+} or Al^{3+} ions flushed to the surface of the AZ91D anode could react to form zinc or aluminium oxides or hydroxides and finally deposit on the AZ91D surface. These products can provide a certain degree of protection for the AZ91D surface. Therefore, the galvanic current of the AZ91D becomes smaller, as if the surface of AZ91D is "passivated" by the corrosion products from the cathodes.

However, the postulated "passivation effect" is not applicable to the "5steel–5Mg" test panel in the "Mc/Mg" exposure configuration, In this configuration, the galvanic current is even larger. There is no doubt that the cathode steel can be corroded and the dissolved ferrous or ferric ions would be flushed to the anode AZ91D surface in the "Mc/Mg" exposure configuration, and ferrous ions would soon be oxidised into ferric ions because of the presence of oxygen in the salt solution. Fig. 14 demonstrates that the influence of ferric ions on the polarisation of AZ91D is much more significant than for either ZnO and $Al(OH)_3$. The polarisation curve for the AZ91D anode in the $FeCl_3$ containing salt solution is characterised by a straight line over a large potential or current region compared to that seen in the ferric ion free solution. There are two possible explanations for the linear polarisation behaviour. First, the high resistivity

of the solution and hence the high ohmic drop across the solution is dominating the polarisation process. Second, AZ91D becomes extremely active and the polarisation resistance of AZ91D becomes extremely low. The first possibility is unlikely, because the addition of a small amount of $FeCl_3$ can only increase the conductivity rather than the resistivity of the solution. The second possibility could be more practical. It is well known that iron is a detrimental impurity in magnesium alloys and it can significantly accelerate the corrosion of magnesium alloys. In a Fe^{3+} containing solution, there could be a possibility that magnesium is oxidised by the ferric ions with the iron ions being reduced into iron which deposits on the magnesium surface. As a result, the impurity level on the magnesium surface could increase, resulting in a highly active surface and extremely low polarisation resistance.

Decreased polarisation resistance of AZ91D should be responsible for the higher galvanic current of the "5steel–5Mg" test panel in the "Mc/Mg" exposure configuration. According to Eq. (1), even though the difference between E_c and E_a is smaller for the "5steel–5Mg" test panel in the "Mc/Mg" exposure configuration, the galvanic current can still increase if the average polarisation resistance R_a is significantly reduced. This could be the case of the "5steel–5Mg" panel in the "Mc/Mg" exposure configuration. The worsening of galvanic corrosion by the corrosion products from the steel cathode behaves as if the AZ91D surface is "poisoned" by the steel corrosion products.

The influence of the exposure configuration on galvanic corrosion signifies that, in practice even if direct contacts are unavoidable, galvanic corrosion may still be slightly moderated by adjusting the relative positions of the anode and cathode.

3.6. "Shortcut" effect

In a few tests, an AZ91D plate far away from its coupling cathode had a considerable current, even higher than the plates close to the cathode, particularly after several days of salt spray testing. In these cases, the current density did not decrease steadily with the distance from the "anode|cathode" junction, but was abnormally distributed across the test panel surface. Careful examination of the test panel revealed that this was caused by the corrosion products built up between this AZ91D plate and the coupling cathode. The corrosion products provide a highly conductive path (compared with the thin wet film on the test panel surface) for the galvanic current from this AZ91D plate to the coupling cathode, so the galvanic current is high at the AZ91D plate.

Fig. 15 is an example of the "shortcut" effect. The fourth current point (circled in Fig. 15) on the AZ91D side of the "5Al–5Mg" test panel is unexpectedly higher than the third point. Observation of the surface of test panel after salt spray testing confirmed that corrosion products had accumulated at the bottom of the test panel (Fig. 16). The corrosion products created a "shortcut" from the fourth AZ91D plate (counted from the anode|cathode junction) to the aluminium plates. A thicker and more continuous solution path can be easily formed along such a "shortcut" significantly reducing the solution resistance between the AZ91D plate and the aluminium plates.

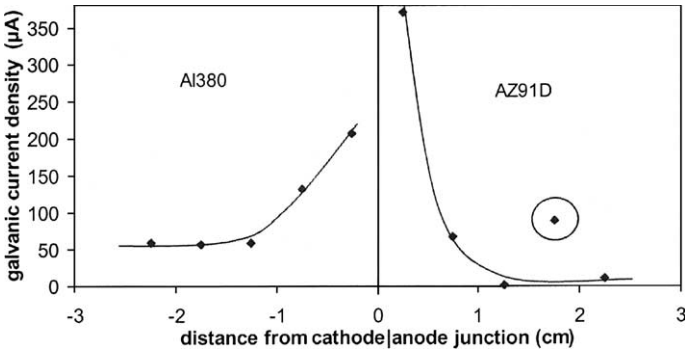

Fig. 15. An abnormal current density point (circled in the figure) on a "5Al–5Mg" test panel in the "Mc|Mg" exposure configuration after exposure to salt spraying for 3 days.

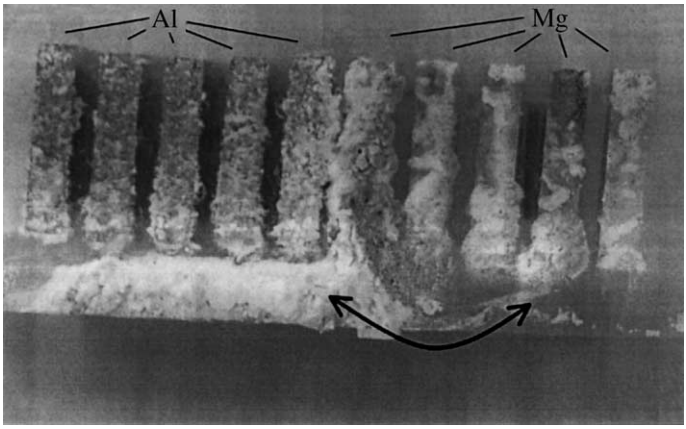

Fig. 16. Corrosion products building up a "shortcut" on a "5Al–5Mg" test panel in the "Mc|Mg" exposure configuration under the salt spraying condition.

The "shortcut" effect observed in the laboratory implies that in practice galvanic corrosion could eventually occur even though the possibility of this type of corrosion appears unlikely at the beginning. In real service environments, not only the corrosion products, but many other substances, such as mud, can also build up a "shortcut" to initiate or accelerate the galvanic corrosion process.

4. Conclusions

1. The galvanic corrosion rate of AZ91D in contact with zinc, Al380 or steel 4150 in general increases with time, i.e., galvanic corrosion will become more severe over time once it is initiated.

2. The area of serious galvanic corrosion on AZ91D adjacent to the cathode is relatively narrow compared to the galvanically protected area on the coupling cathode. However, the galvanically affected zone can be relatively large and galvanic corrosion may be caused by a remote cathode metal.
3. Within a certain range, increasing the ratio of cathode area to anode area leads to an increase in the galvanic corrosion rate. A large steel, zinc or aluminium component coupled with a small AZ91D component should be avoided in practice. Otherwise severe galvanic corrosion will result.
4. Increasing the thickness of the insulating spacer between AZ91D and its coupling can significantly reduce the rate of galvanic corrosion. However, galvanic corrosion cannot be eliminated by simply increasing the thickness of an insulating spacer if AZ91D is still electrically connected to the cathode metal.
5. Steel is the worst of the three cathode metals studied in terms of the galvanic corrosion rate, the distribution of galvanic current density and the influence of the cathode/anode area ratio, while aluminium causes the least corrosive attack to the AZ91D alloy.
6. The relative positions of magnesium and its coupling cathode also affect the galvanic corrosion process. If the corrosion products from the AZ91D anode can be transferred to the cathode, e.g., when AZ91D is placed on the top of the cathode, then the galvanic corrosion could be slightly reduced through an ''alkalisation effect''.
7. If the corrosion products from the cathodes are transferred to the surface of AZ91D, then there could be a ''passivation'' effect or ''poisoning effect'', which could either slightly ameliorate or deteriorate the galvanic corrosion. Al380 and Zn cathodes may have a ''passivation effect'' and steel 4150 may have a ''poisoning effect''.
8. A ''shortcut'' effect can be caused by the accumulation of corrosion products, which can accelerate galvanic corrosion unexpectedly at a remote area.

Acknowledgements

The study was supported by the CRC for Cast Metals Manufacturing (CAST). CAST was established under and is supported by the Australian Government's Cooperative Research Centres Program (CRC). It is also acknowledged that Mr. Gary Cleeland assisted in the galvanic current measurements.

References

[1] A. Wichberg, R. Ericsson, Magnesium in the LCP 2000, SAE technical paper 850418, 1995.
[2] R. Melde, Volvo LCP Light Component Project, SAE technical paper 850570, 1995.
[3] M. Isacsson, H. Rootzen, O. Lunder, Galvanically induced atmospheric corrosion on magnesium alloys: a designed experiment evaluated by extreme value statistics and conventional techniques, SAE, SP-1250, No. 970328, 1997, pp. 43–55.

[4] ASTM G82-98, Standard guide for development and use of a galvanic series for predicting galvanic corrosion performance, ASTM 3.02, 1998, pp. 356–361.
[5] Harvey P. Hack (Ed.), Galvanic Corrosion, STP 978, ASTM, 1988.
[6] C. Wagner, Journal of the Electrochemical Society 98 (1951) 116.
[7] J.T. Waber, Journal of the Electrochemical Society 101 (1954) 271.
[8] A. Tahara, T. Kodama, Corrosion Science 42 (2000) 655.
[9] J.T. Waber, M. Rosenbluth, Journal of the Electrochemical Society 102 (1955) 344.
[10] J.T. Waber, Journal of the Electrochemical Society 102 (1955) 220.
[11] E. Kennard, J. Waber, Journal of the Electrochemical Society 117 (1970) 880.
[12] L. Gal-Or, Y. Raz, J. Yahalon, Journal of the Electrochemical Society 120 (1973) 598.
[13] E. McCafferty, Corrosion Science 16 (1976) 183.
[14] E. McCafferty, Journal of the Electrochemical Society 124 (1977) 1869.
[15] P.H. Melville, Journal of the Electrochemical Society 126 (1979) 2081.
[16] P.H. Melville, Journal of the Electrochemical Society 127 (1980) 864.
[17] J.A Klingert, S. Lynne, C.W. Tobias, Electrochimica Acta 9 (1964) 297.
[18] P. Doig, P.E.J. Flewitt, Journal of the Electrochemical Society 126 (1979) 2057.
[19] J.W. Fu, Corrosion 38 (1982) 295.
[20] R. Sautebin, H. Froidewaux, D. Landolt, Journal of the Electrochemical Society 127 (1980) 1096.
[21] H.P.E. Helle, G.H.M. Beck, Ligtelijin, Corrosion 37 (1981) 522.
[22] R.G. Kasper, M.G. April, Corrosion 39 (1983) 181.
[23] R.S. Munn, Materials Performance August (1982) 29.
[24] R.S. Munn, O.F. Devereux, Corrosion 47 (1991) 612.
[25] R.S. Munn, O.F. Devereux, Corrosion 47 (1991) 618.
[26] M. Miyaska, K. Hashimoto, K. Kishimoto, S. Aoki, Corrosion Science 30 (1990) 299.
[27] S. Aoki, K. Kishimoto, Mathematical and Computer Modelling 15 (1991) 11.
[28] H.P. Hack, Corrosion Review 15 (1997) 195.
[29] Gungling Song, A. Atrens, Corrosion of magnesium alloys (invited refereed review article), in: Corrosion and Environmental Degradation of Materials, Materials Science and Technology, vol. 19, Wiley-VCH Verlag GmbH, 2000.
[30] G.L. Makar, J. Kruger, Corrosion of magnesium, International Materials Reviews 38 (1993) 138.
[31] M. Starostin, A. Smorodin, Y. Cohen, L. Gal-Or, S. Tamir, Galvanic corrosion of magnesium alloys, in: E. Aghion, D. Eliezer (Eds.), Magnesium 2000, Proceedings of the Second Israeli International Conference on Magnesium Science and Technology, Dead Sea, Israel, 2000, pp. 363–370.
[32] G. Gao, G. Cole, M. Richetts, J. Balzer, P. Frantzeskakis, Effects of fastener surface on galvanic corrosion of automotive magnesium components, in: E. Aghion, D. Eliezer (Eds.), Magnesium 2000, Proceedings of the Second Israeli International Conference on Magnesium Science and Technology, Dead Sea, Israel, 2000, pp. 321–338.
[33] D.L. Hawke, Galvanic corrosion of magnesium, SDCE 14th International Die Casting Congress and Exposition, Toronto, Canada, May 1987, Paper No. G-T87-004.
[34] J. Senf, E. Broszeit, M. Gugau, C. Berger, Corrosion and galvanic corrosion of die casted magnesium alloys, in: H.I. Kaplan, J. Hryn, B. Clow (Eds.), Magnesium Technology 2000, TMS, Nashville, 2000, pp. 137–142.
[35] J.I. Skar, Materials and Corrosion 50 (1999) 2.
[36] E. Boese, J. Gollner, A. Heyn, J. Strunz, Materials and Corrosion 52 (2001) 247.
[37] H.O. Teeple, Atmospheric galvanic corrosion of magnesium coupled to other metals, ASTM, STP 175, 1956, pp. 89–115.
[38] X.G. Zhang, Journal of the Electrochemical Society 143 (1996) 1472.
[39] M. Stratmann, H. Streckel, Corrosion Science 30 (1990) 681.
[40] H.P. Hack, Galvanic, in: R. Baboian (Ed.), Corrosion Tests and Standards: Application and Interpretation, ASTM Manual Series: MNL 20, 1995, pp. 86–196.
[41] C. Wagner, Journal of Electrochemical Society 98 (1951) 116.
[42] H. Hack, Materials Performance 18 (1989) 72.
[43] J.R. Scully, H.P. Hack, Prediction of tube-tubesheet galvanic corrosion using finite element and Wagner number analyses, in: H.P. Hack (Ed.), Galvanic Corrosion, ASTM, 1988, pp. 136–157.

[44] C.B. Baliga, P. Tsakiospolous, Design of magnesium alloys with improved corrosion properties, in: Conference Proceedings Garmich Partenkirchen, April 1992, pp. 119–126.
[45] R.S. Busk, Magnesium Products Design, Marcel Dekker, 1987, pp. 497–499.
[46] Handbook of Chemistry and Physics, 57th ed., CRC Press Inc, 1976–1977, pp. B-127–B-129.